# Single-Mode 1.27-$\mu$m InGaAs:Sb-GaAs-GaAsP Quantum Well Vertical Cavity Surface Emitting Lasers

Hao-Chung Kuo, *Member, IEEE*, Ya-Hsien Chang, Yi-An Chang, Fang-I. Lai, Jung-Tang Chu, Min-Ying Tsai, and Shing-Chung Wang, *Member, IEEE*

***Abstract*—The 1.27-$\mu$m InGaAs:Sb-GaAs-GaAsP vertical cavity surface emitting lasers (VCSELs) were grown by metalorganic chemical vapor deposition and exhibited excellent performance and temperature stability. The threshold current varies from 1.8 to 1.1 mA and the slope efficiency falls less than $\sim$35% from 0.17 to 0.11 mW/mA as the temperature is raised from room temperature to 75 °C. The VCSELs continuously operate up to 105 °C with a slope efficiency of 0.023 mW/mA. With a bias current of only 5 mA, the 3-dB modulation frequency response was measured to be 8.36 GHz, which is appropriate for 10-Gb/s operation. The maximal bandwidth is estimated to be 10.7 GHz with modulation current efficiency factor of $\sim$ 5.25 GHz/(mA)$^{1/2}$. These VCSELs also demonstrate high-speed modulation up to 10 Gb/s from 25°C to 70°C. We also accumulated life test data up to 1000 h at 70°C/10 mA.**

***Index Terms*—Characterization, InGaAsSb, laser diodes, metalorganic chemical vapor deposition (MOCVD), optical fiber devices, semiconducting.**

## I. Introduction

LONG-WAVELENGTH vertical cavity surface-emitting lasers (VCSELs) are key devices in optical fiber metropolitan-area networks (MANs) [1]. The most promising results regarding low-cost long-wavelength lasers or VCSELs, have been obtained using GaInAsN quantum wells (QWs) grown on GaAs substrates [1]–[7]. The large conduction band offset improves the temperature performance over that of conventional InP-based materials. The GaAs system provides high-performance AlGaAs/GaAs DBR mirrors and permits the use of the well-established oxide-confined GaAs-based VCSEL manufacturing infrastructure. However, GaInAsN is a very challenging material system from a growth perspective: 1) incorporating N into the InGaAs QW is difficult and increases the nonradiative (monomolecular and Auger) recombination, reducing the material gain and increasing the transparency carrier density [8]; 2) during post-growth annealing, the nitrogen diffuses out from the quantum well and blue-shifts the optical emission. Recently, Koyama *et al.* [9] and Tansu *et al.* [10] employed highly strained InGaAs QW active lasers to extend the emission wavelength to 1.2 $\mu$m. Highly strained InGaAs VCSELs with a photoluminescence (PL) peak at 1.205 $\mu$m and a laser emission wavelength of $\sim$ 1.26–1.27 $\mu$m have demonstrated a promising performance and continuous-wave (CW) operation at up to 120 °C as well as 10 Gb/s operation [11]. However, the emission wavelength of 1.26 $\mu$m barely meets optical communication standards, such as IEEE 820.3ae 10 Gb/s Ethernet. Furthermore, this laser performs relatively poor at room temperature due to the large negative gain-cavity offset. Antimony (Sb) present during GaInAsN growth has been believed to act as a surfactant and improve PL performance [12]. The authors have observed that adding Sb into samples with high In content sharply increases the intensity and the alloy thus formed exhibits significant red-shift in optical emission [12]. Additionally, adding a surfactant such as Sb [13] or Te [14] significantly increases the critical layer thickness of InGaAs on GaAs. This work presents high-performance InGaAs:Sb-GaAs-GaAsP QWs VCSELs grown by metal organic chemical vapor deposition. These VCSELs exhibit excellent performance and temperature stability. The threshold current changes from 1.8 to 1.1 mA and the slope efficiency falls less than $\sim$35% from 0.17 to 0.11 mW/mA as the temperature is raised from room temperature to 75 °C. The VCSELs continuously operate up to 105 °C with a slope efficiency of 0.023 mW/mA. With a bias current of only 5 mA, the 3-dB modulation frequency response is measured to be 8.36 GHz, which is suitable for 10 Gb/s operation. The maximal bandwidth is $\sim$10.7 GHz with MCEF of $\sim$ 5.25 GHz$/(\mathrm{mA})^{1/2}$.

## II. Structure and Physical Model

All structures were grown on semi-insulating GaAs (100) substrates by low pressure metalorganic chemical vapor deposition. The group-V precursors were the hydride sources $AsH_3$ and $PH_3$. The trimethyl alkyls of gallium (Ga), aluminum (Al), indium (In), and Antimony (Sb) were the group-III precursors. The epitaxial structure was as follows (from bottom to top)—$n^+$ – GaAs buffer, 40.5-pair $n^+$ – $Al_{0.9}Ga_{0.1}As/n^+$ – GaAs (Si-doped) distributed Bragg reflector (DBR), undoped active region, p – $Al_{0.98}Ga_{0.02}As$ oxidation layer, 25-pair $p^+$ – $Al_{0.9}Ga_{0.1}As/p^+$ – GaAs DBR (carbon-doped) and $p^+$ – GaAs (carbon-doped) contact layer. The graded-index separate confinement heterostructure

Manuscript received July 15, 2004; revised October 26, 2004. This work was supported in part by the National Science Council of the Republic of China in Taiwan under Contract NSC 90-2215-E-009-102, in part by the Academic Excellence Program of the ROC Ministry of Education under Contract 88-FA06-AB, and in part by .the Institute of Nuclear Energy under Contract 922001InER015.

The authors are with the Institute of Electro-Optical Engineering, National Chiao-Tung University, Hsinchu 300, Taiwan, R.O.C. (e-mail: hckuo@faculty.nctu.edu.tw).

Digital Object Identifier 10.1109/JSTQE.2004.841696

1077-260X/$20.00 © 2005 IEEE

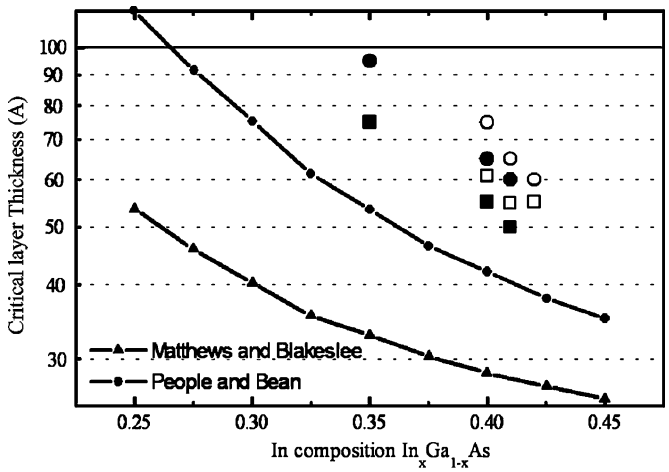


Fig. 1. Numerical calculation of the critical thickness for $In_xGa_{1-x}As-GaAs$ as a function of indium composition x in the range $0.25 < \times < 0.45$. Full symbols represent the QWs where there defects were not observed. Open symbols indicate that QWs show faceting or dislocations. Square symbols represent InGaAs grown on GaAs, while circle symbols represent InGaAs grown on GaAs with $\sim$1.5% Sb incorporation.

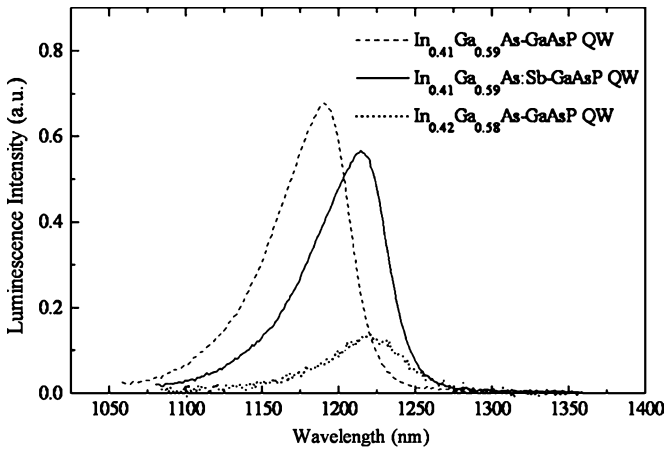


Fig. 2. Comparison of the photoluminescence spectra of InGaAs with different In composition and $In_{0.41}Ga_{0.59}As$ with Sb incorporation.

(GRINSCH) active region consisted mainly of a double QWs active region $In_{0.41}Ga_{0.59}As : Sb - GaAs - GaAs_{0.85}P_{0.15}$ (60/100/100 Å), with PL emission at 1.214 $\square\mu$m, embedded between two linear-graded $Al_xGa_{1-x}As$ (x = 0 to 0.6 and x = 0.6 to 0) confinement layers (growth temperature = 550 °C with $AsH_3$/TMSb flow ration ~50). The cavity was formed in one-wavelength thickness. Carbon was used as the $p$-type dopant in the DBR to increase the carrier concentration $(2 - 3 \times 10^{18}$ cm$^{-3})$. The interfaces of both $p$- and $n$-type $Al_{0.9}Ga_{0.1}As$/GaAs DBR layers are linearly graded to reduce the series resistance. The growth rate is $\sim$ 1 $\mu$m/hr for InGaAs:Sb QW region and $\sim$ 2 $\mu$m/hr for $Al_{0.9}Ga_{0.1}As$/GaAs DBR region. The optical properties of QWs were optimized through PL measurement and structural analysis as described as followed. The FP-dip wavelength is at 1270 nm, which was determined by reflection measurement.

To optimize growth parameters, we need to investigate critical layer thickness (CLT) of InGaAs grown on GaAs with the effect of Sb surfactant. In lattice-mismatched systems, the strain of the layers is accommodated elastically in layers thinner than a misfit-dependent critical thickness as described by Matthews and Blakeslee [15]. Fig. 1 shows the numerical calculation of the critical thickness for $In_xGa_{1-x}As - GaAs$ as a function of indium composition x in the range $0.25 < x < 0.45$. Substituting the critical thickness as a function of Indium composition for the width of the quantum well, the energy states are calculated for the first level in the QW. The maximal achievable wavelength is less than 1100 nm. However, recent publication demonstrated that the critical thickness of InGaAs on GaAs is larger than Matthews and Blakeslee's predication and the maximal wavelength can be achieved is ~1200 nm [16], [17]. People and Bean have proposed an alternative description for the critical thickness by defining a balance between the strain energy in an epitaxial layer and the formation energy of an isolated screw dislocation [18]. Additionally, the critical thickness of InGaAs on GaAs can be enhanced by additional strain compensating layer or surfactant [13]. Secondary Ion mass spectroscopy (SIMS) measurement was performed to investigate whether Sb being incorporated into the lattice or just as a surfactant while the TEM measurements were used to determine the formation of faceting or dislocations. This critical thickness is plotted in Fig. 1. Full symbols represent the QWs where the defects were not observed. Open symbols indicate that QWs show faceting or dislocations. Square symbols represent InGaAs grown on GaAs, while circle symbols represent InGaAs grown on GaAs with ~1.5% Sb incorporation (measured by SIMS). It is clear that the Sb do incorporate into the crystal and the CLT of InGaAs on GaAs increases with adding of Sb. No dislocations were observed for 75 Å $In_{0.4}Ga_{0.6}As : Sb/GaAs$, 60 Å $In_{0.41}Ga_{0.59}As : Sb/GaAs$ and 50 Å $In_{0.42}Ga_{0.58}As : Sb/GaAs$ QWs. These results are consistent with the observations of [13].

Fig. 2 compares the PL spectra of $In_xGa_{1-x}As$ QW with various In contents (x = 0.41 and 0.42), and that of $In_{0.41}Ga_{0.59}As$ QW with incorporated Sb. All samples have a well thickness of 60 Å with a GaAs spacer and a $GaAs_{0.85}P_{0.15}$ strain-compensating layer. The PL peak emission wavelengths $(\lambda_p)$ of the grown $In_{0.41}Ga_{0.59}As/GaAs/GaAsP$ and $In_{0.41}Ga_{0.59}As : Sb/GaAs/GaAsP$ QWs are 1.194 and 1.214 $\mu$m, respectively. A red-shift of 20 nm is observed. For $In_{0.41}Ga_{0.59}As : Sb$, the full-width at half-maximum (FWHM) of the PL emission peak from $In_{0.41}Ga_{0.59}As : Sb$ is larger and the PL intensity is slightly lower. The red-shift of InGaAs:Sb can be attributed to the Sb in the alloy constituent. The incorporation of more indium or the lowering of the conduction band also explains the red-shift of the optical emission. The FWHM of the PL emission increases significantly and the PL intensity drops dramatically when the indium composition increases to 0.42. These changes can be explained by the dislocations and the formation of nonradiative defects of the 60 Å $In_{0.42}Ga_{0.0.58}As/GaAs/GaAsP$ QW where 60 Å exceeds the critical layer thickness. From the reflectivity spectrum of an as-grown VCSEL structure, the cavity mode is centered at 1.266 $\mu$m and the stop band is over 90 nm which is due to the large index contrast of AlGaAs/GaAs DBRs. The cavity mode and the gain mode offset is determined to be 52 nm.

Fig. 3 schematically depicts the VCSEL structure. A processing sequence involved six photomasks to fabricate oxide-

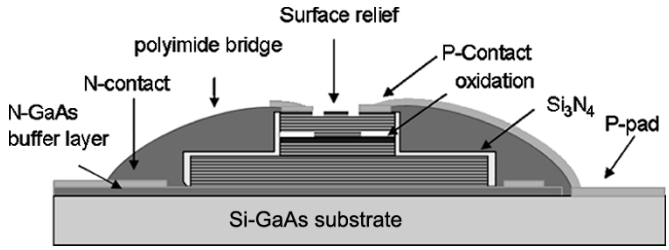


Fig. 3. Schematic cross section of high speed VCSEL structure. The oxide-confined aperture is 5 $\mu$m and the surface relief size is 3.5 $\mu$m.

confined polyimide-planarized VCSELs with coplanar waveguide probe pads. This process was designed to minimize capacitance while keeping a reasonably low resistance [19]. Device fabrication began with the formation of cylindrical mesas with a diameter of 30 $\mu$m by etching the surrounding semiconductor into the bottom $n$-type mirror to a depth of 5 $\mu$m, using an ICP-RIE system. The sample was wet-oxidized in a 420 °C steam environment for 20 min to form the current aperture and provide lateral index guiding to the lasing mode. The oxidation rate was 0.6 $\mu$m/ min for the $Al_{0.98}Ga_{0.02}As$ layer, so the oxide extended 12.5 $\mu$m from the mesa sidewall. Ti/Au was evaporated to form the p-type contact ring, and AuGeNiAu was evaporated onto the etched n-buffer layer to form the n-type contact, which is connected to the semi-insulating substrate. Contacts were alloyed for 30 s at 420 °C with rapid thermal annealing (RTA). After the contact formation, the photosensitive polyimide was spun on the sample to form insulation and planarization. Ti-Au was deposited to a thickness of from 200 to 3000 Å to form the metal interconnects and coplanar waveguide probe pads. Heat treatment following metal deposition was applied to strengthen the metal-to-polyimide adhesion. Finally, surface relief etching with a diameter of 3.5 $\mu$m was performed to a depth of near half wavelength for single-mode operation [20].

## III. Results and Discussions

The DC characteristics of completed VCSELs were measured with a probe station, an Agilent 4145 A semiconductor parameter analyzer and an InGaAs photodiode. Fig. 4 plots curves of temperature-dependent light output and voltage versus current (LIV). The maximal output power exceeds 1.2 mW at room temperature (0.4 mW at 95 °C) and output power rollover occurs as the current increases above 10 mA at 25 °C (8.7 mA at 95 °C). Furthermore, a large drop in the maximal power was observed in the temperature range between 75 °C $\sim$ 95 °C. The large drop in maximal power might be resulted from the higher free carrier absorption and higher Auger recombination rate in high temperature. Improvement in output power might be achieved by 1) optimizing the doping profile in the cavity region and 2) further pushing the emission wavelength longer to reduce the cavity-gain detuning.

The threshold current and slope efficiency were plotted as a function of heat sink temperature, as shown in Fig. 5. The large cavity-gain offset resulted in decreasing threshold current densities as the temperature was increased. When the gain maximum and the emission wavelength were aligned, a minimum threshold current of $\sim$1.1 mA was achieved at $\sim$70 °C–75 °C.

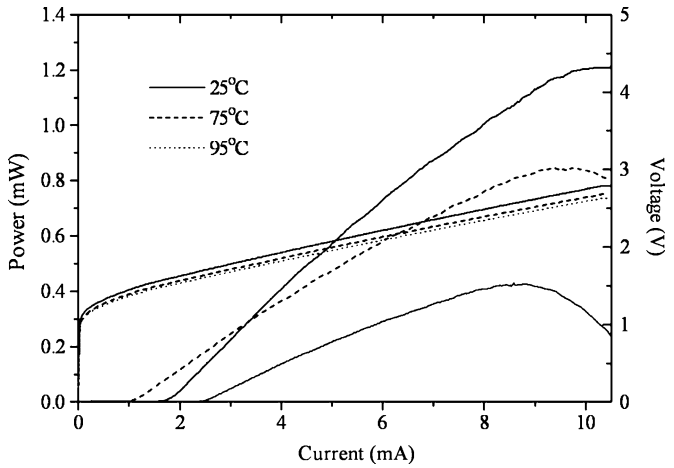


Fig. 4. Temperature-dependent light output and voltage versus current (LIV) curves.

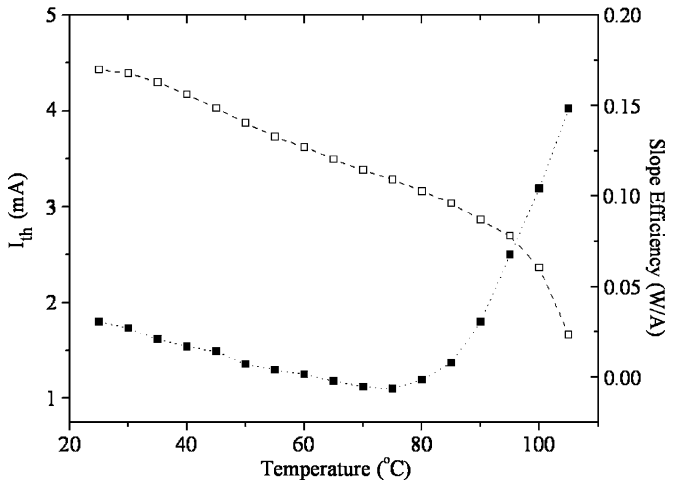


Fig. 5. Threshold current and slope efficiency as a function of heat sink temperature.

The slope efficiency was 0.17 mW/mA at room temperature and fall less than $\sim$35% as the temperature was raised to 75 °C. The VCSEL's continuously operated up to 105 °C with a slope efficiency of 0.023 mW/mA. The resistance of the VCSEL is $\sim$ 120 $\Omega$ and the capacitance is $\sim$0.1 pF. Accordingly, parasitic effects limit the devices to a frequency response of $\sim$13 GHz.

Lateral mode characteristic is an important feature for long wavelength VCSELs since it strongly affects the transmission properties, especially the long haul optical communication. The spectra of the InGaAs:Sb-GaAs-GaAsP VCSELs were measured using an Advantest Q8381 A optical spectrum analyzer with a resolution of $\sim$0.1 nm. The devices exhibit single transverse mode characteristics at a lasing wavelength of $\sim$ 1.27 $\mu$m, with a side mode suppression ratio (SMSR) of $>$30 dB over the whole operating range, as depicted in Fig. 6.

The small signal response of VCSELs as a function of bias current was measured using a calibrated vector network analyzer (Agilent 8720 ES) with wafer probing and a 50 $\mu$m multimode optical fiber connected to a New Focus 25 GHz photodetector. Fig. 7 indicates the modulation bandwidth increases with the bias current, until it flattens at a bias of about 7 mA. At

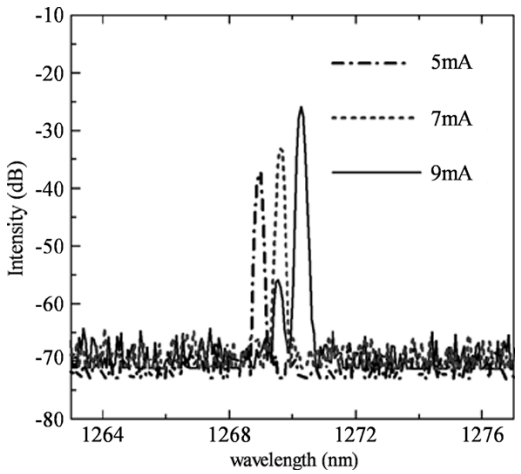


Fig. 6. Emission spectra of InGaAs:Sb-GaAs-GaAsP VCSELs at different driving currents.

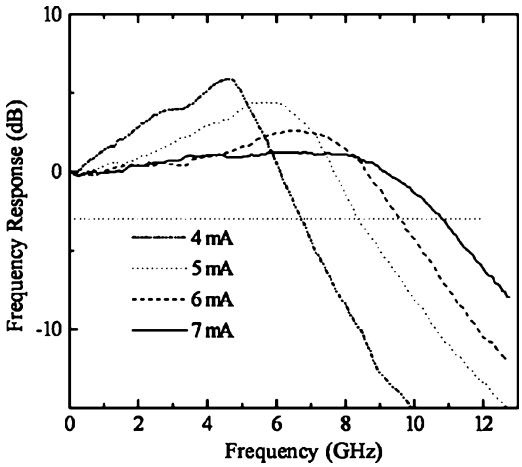


Fig. 7. Small signal modulation measurement on InGaAs:Sb-GaAs-GaAsP VCSELs.

a bias current of only 5 mA, the maximum 3-dB modulation frequency is measured as 8.36 GHz, which is suitable for 10 Gb/s operation. In Fig. 8, the 3-dB bandwidth $(f_{3\,dB})$ is plotted as a function of the bias current. At low-bias currents, the bandwidth increase in proportion to the square root of the current above threshold, as expected from the rate equation analysis. The saturation of bandwidth was clear observed as bias current increases above 7 mA which can be attributed to heating effect. The maximal bandwidth is estimated to 10.7 GHz with modulation current efficiency factor (MCEF) of $\sim 5.25\ \mathrm{GHz}/(\mathrm{mA})^{1/2}$.

To measure the high-speed VCSEL under large signal modulation, microwave and light wave probes were used in conjunction with a 10 Gb/s pattern generator (MP1763 Anritsu) with a pseudorandom bit sequence of $2^{23}-1$ and a 12.5-GHz photoreceiver with an OC-192 low pass filter. Eye diagrams were obtained for back-to-back (BTB) transmission on VCSELs. Fig. 9(a) demonstrates that the room temperature eye diagram of the presented VCSEL biased at 6 mA, with data up to 10 Gb/s and an extinction ratio of 6 dB. The clear open eye pattern indicates good performance of these InGaAs:Sb VCSELs with the rise time $(T_r)$ of 30 ps, the fall time $(T_f)$

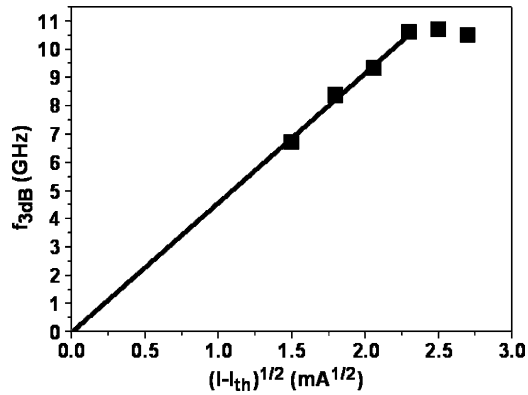


Fig. 8. The 3-dB bandwidth $(f_{3\,dB})$ is plotted as a function of the bias current.

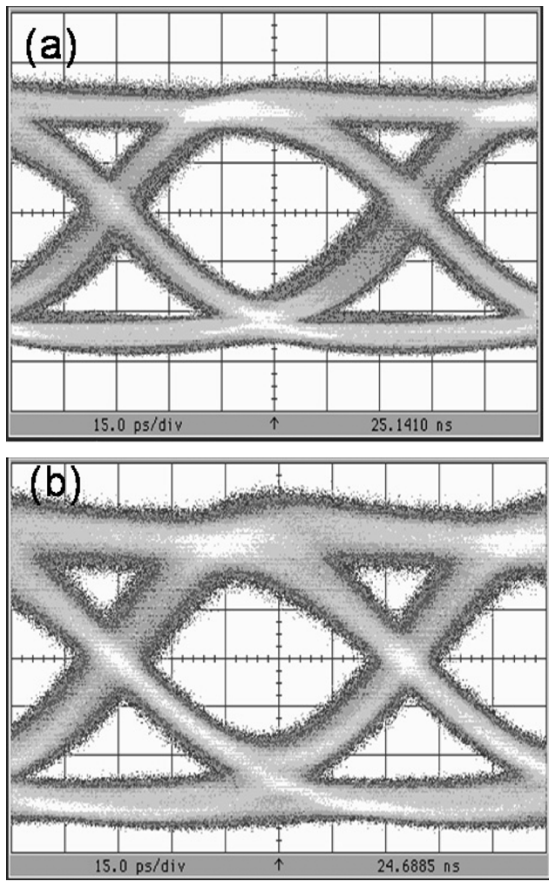


Fig. 9. (a) Room temperature (b) 70 °C eye diagram of our VCSEL data up to 10 Gb/s and 6 dB extinction ratio. The scale is 15 ps/div.

of 41 ps, and jitter (p-p) <20 ps. The VCSELs also exhibit superior performance at high temperature. The reasonably open eye-diagram in Fig. 9(b) demonstrates the high-speed performance of the VCSEL (biased at 7 mA) at 10 Gb/s with an extinction ratio of 6 dB at 70 °C. This result further verifies the superior performance of the presented VCSELs.

To guarantee the device reliability is always a tough work but a natural task for the components supplier in the data communication markets. We have accumulated life test data up to 1000 h at 70 °C/10 mA. As shown in Fig. 10, the threshold current is plotted versus time scale for the InGaAs:Sb VCSEL chips on TO-46 header under the high temperature operation lifetime

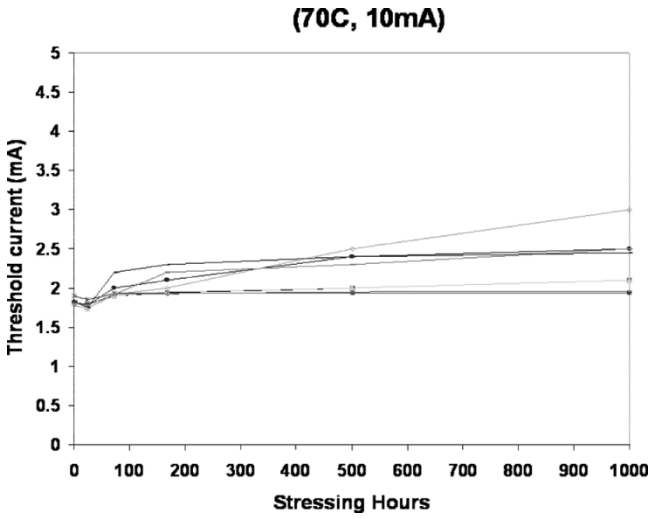


Fig. 10. HTOL (70 °C/10 mA) performance of the InGaAs:Sb-GaAs-GaAsP VCSEL.

(HTOL) test at 70 °C/10 mA. The threshold current was drop slightly at first 72 h which might be attributed to initial material stability. All samples show pretty stable performance except one sample show slight degradation after 1000 h.

## IV. Conclusion

High-performance InGaAs:Sb-GaAs-GaAsP QWs VCSELs with an emission wavelength of 1.27 $\mu$m were successfully demonstrated. The VCSEL's exhibit a very low threshold current, good temperature performance, and a high modulation bandwidth of $\sim$ 10.7 GHz with MCEF of $\sim$ 5.25 GHz$/(\text{mA})^{1/2}$. The VCSELs also demonstrate high-speed modulation up to 10 Gb/s from 25 °C to 70 °C. The results reveal the performance of the InGaAs:Sb VCSELs comparable to that of GaInAsN VCSELs, but with better thermal stability. They are, therefore, very promising candidates for 1.3 $\mu$m commercial applications.

## Acknowledgment

The authors would like to thank Dr. C. Kuo of LuxNet Corporation, Dr. C. H. Lin of Agilent Technologies, Dr. C. P. Sung and Dr. J. Chi of ITRI, and Prof. N. Tansu of Lehigh University for useful discussions and technical support.

## References

[1] M. Tan, "Progress in long wavelength VCSELs," in *Proc. Lasers Electro-Optics Soc., 15th Annu. Meet. IEEE*, vol. 1, 2002, pp. 269–270.

[2] M. Kondow, T. Kitatani, S. Nakatsuka, M. C. Larson, K. Nakahara, Y. Yazawa, M. Okai, and K. Uomi, "GaInNAs: A novel material for long-wavelength semiconductor lasers," *IEEE J. Select. Topic Quantum Electron.*, vol. 3, no. 3, pp. 719–730, Jun. 1997.

[3] C. W. Tu and P. Yu, "Material properties of III-V semiconductors for lasers and detectors," *MRS Bull.*, vol. 28, pp. 345–349, 2003.

[4] C. W. Tu, "III-N-V low bandgap nitrides and their device applications," *J. Phys:Condens. Matter*, vol. 13, pp. 7169–7182, 2001.

[5] K. D. Choquette, J. F. Klem, A. J. Fischer, O. Blum, A. A. Allerman, I. J. Fritz, S. R. Kurtz, W. G. Breiland, R. Sieg, K. M. Geib, J. W. Scott, and R. L. Naone, "Room temperature continuous wave InGaAsN quantum well vertical-cavity lasers emitting at 1.3 $\mu$m," *Electron. Lett.*, vol. 36, no. 16, pp. 1388–1390, 2000.

[6] T. Takeuchi, Y.-L. Chang, M. Leary, A. Tandon, H.-C. Luan, D. Bour, S. Corzine, R. Twist, and M. Tan, "1.3-$\mu$m InGaAsN vertical cavity surface emitting lasers grown by MOCVD," *Electron. Lett.*, vol. 38, pp. 1438–1440, 2002.

[7] M. Kawaguchi, T. Miyamoto, E. Gouardes, D. Schlenker, T. Kondo, F. Koyama, and K. Iga, "Lasing characteristics of low-threshold GaInNA's lasers grown by metalorganic chemical vapor deposition," *Jpn. J. Appl. Phys.*, vol. 40, pp. L744–L746, 2001.

[8] N. Tansu and L. J. Mawst, "Temperature sensitivity of 1300-nm InGaAsN quantum-well lasers," *IEEE Photon. Technol. Lett.*, vol. 14, pp. 1052–1054, 2002.

[9] F. Koyama, D. Schlenker, T. Miyamoto, Z. Chen, A. Matsutani, T. Sakaguchi, and K. Iga, "1.2 $\mu$m highly strained GaInAs/GaAs quantum well lasers for single mode fiber datalink," *Electron. Lett.*, vol. 35, no. 13, pp. 1079–1081, 1999.

[10] N. Tansu, J. Y. Yeh, and L. J. Mawst, "Extremely-low threshold-current-density InGaAs quantum well lasers with emission wavelength of 1215–1233 nm," *Appl. Phys. Lett.*, vol. 82, no. 23, pp. 4038–4040, 2003.

[11] P. Sundgren, R. M. von Wurtemberg, J. Berggren, M. Hammar, M. Ghisoni, V. Oscarsson, E. Odling, and J. Malmquist, "High-performance 1.3-$\mu$m InGaAs vertical cavity surface emitting lasers," *Electron. Lett.*, vol. 39, pp. 1128–1129, 2003.

[12] V. Gambin, H. Wonill, M. Wistey, Y. Homan, S. R. Bank, S. M. Kim, and J. S. Harris, "GaInNAsSb for 1.3–1.6 $\mu$m-long wavelength lasers grown by molecular beam epitaxy," *IEEE J. Select. Topic Quantum Electron.*, vol. 8, no. 4, pp. 795–800, Jul./Aug. 2002.

[13] J. C. Harmand, L. H. Li, G. Patriarche, and L. Travers, "GaInAs/GaAs quantum-well growth assisted by Sb surfactant: toward 1.3 $\mu$m emission," *Appl. Phys. Lett.*, vol. 84, pp. 3981–3983, 2004.

[14] J. Massies, N. Grandjean, and V. H. Etgens, "Surfactant mediated epitaxial growth of $In_xGa_{1-x}As$ on GaAs (00I)," *Appl. Phys. Lett.*, vol. 61, pp. 99–101, 1992.

[15] J. W. Matthews and A. E. Blakeslee, *J. Crystal Growth*, vol. 27, p. 118, 1974.

[16] N. Tansu, J. Y. Yeh, and L. J. Mawst, "Extremely low threshold-current-density InGaAs quantum-well lasers with emission wavelength of 1215–1233 nm," *Appl. Phys. Lett.*, vol. 82, pp. 4038–4040, 2003.

[17] N. Tansu, Y. L. Chang, T. Takeuchi, D. P. Bour, S. W. Corzine, M. R. T. Tan, and L. J. Mawst, "Temperature analysis and characteristics of highly strained InGaAs-GaAsP-GaAs ($\lambda > 1.17$ $\mu$m) quantum-well lasers," *IEEE J. Quantum Electron.*, vol. 38, no. 6, pp. 640–651, Jun. 2002.

[18] R. People and J. C. Bean, "Calculation of critical layer thickness versus lattice mismatch for $Ge_xSi_{1-x}/Si$ strained-layer heterostructures," *Appl. Phys. Lett.*, vol. 47, pp. 322–325, 1985.

[19] H. C. Kuo, Y. S. Chang, F. Y. Lai, T. H. Hsueh, L. H. Laih, and S. C. Wang, "High-speed modulation of 850 nm InGaAsP/InGaP strain-compensated VCSELs," *Electron. Lett.*, vol. 39, pp. 1051–1053, 2003.

[20] H. J. Unold, S. W. Z. Mahmoud, R. Jäger, M. Grabherr, R. Michalzik, and K. J. Ebeling, "Large-area single-mode VCSELs and the self-aligned surface relief," *IEEE J. Select. Topics Quantum Electron.*, vol. 7, no. 2, pp. 386–392, Mar./Apr. 2000.

**Hao-Chung Kuo** (S'94–M'99), received the B.S. degree in physics from National Taiwan University, Taipei, Taiwan, R.O.C., in 1990, the M.S. degree in electrical and computer engineering from Rutgers University, New Brunswick, NJ, in 1995, and the Ph.D. in electrical and computer engineering from the University of Illinois, Urbana–Champaign, in 1999.

He has an extensive professional career both in research and industrial research institutions. He has been a Research Consultant with Lucent Technologies, Bell Laboratories, Holmdel, NJ, (1995–97); an R&D Engineer with the Fiber-Optics Division, Agilent Technologies, Palo Alto, CA, (1999–2001); and an R&D Manager with LuxNet Corporation, Fremont, CA, (2001–2002). Since September 2002, he has been a Faculty Member with the Institute of Electro-Optical Engineering, National Chiao Tung University, Hsinchu, Taiwan, R.O.C. He has authored or co-authored over 60 publications. His current research interests include the epitaxy, design, fabrication, and measurement of high speed InP and GaAs based vertical cavity surface emitting lasers, as well as GaN-based Lighting emitting devices and nanostructures.

**Ya-Hsien Chang** was born in Taipei, Taiwan, R.O.C., on Jan 12, 1976. He received the B.S. and M.S. degrees in electrical engineering from National Tsing-Hua University, Hsinchu, Taiwan, R.O.C. He is currently working toward the Ph.D. degree at the Institute of Electro-Optical Engineering, National Chiao-Tung University, Hsinchu, Taiwan, R.O.C.

His research is focused on characterizing III-nitride material and modeling the high speed VCSEL's.

**Yi-An Chang** was born in Taipei, Taiwan, R.O.C., on March 13, 1978. He received the B.S. and M.S. degrees in physics from the National Changhua University of Education (NCUE), Changhua, Taiwan, R.O.C., in 2001 and 2003, respectively. He is currently working toward the Ph.D. degree in electrooptical engineering at the Institute of Electro-Optical Engineering, National Chiao-Tung University, Hsinchu, Taiwan, R.O.C.

He joined the Laboratory of Lasers and Optical Semiconductors, NCUE, in 2000, where he was engaged in research on passive $Q$-switching with solid-state saturable absorbers and III-nitride semiconductor materials for light-emitting diodes and semiconductor lasers. His research interests include InGaN and InGaAsN semiconductor lasers.

**Fang-I Lai** was born in Taipei, Taiwan, on October 4, 1975. She received the B.S. degree in physics from Tung-Hai University, Taichung, Taiwan, R.O.C., and the M.S. degree from the Institute of Electro-Optical Engineering, National Chiao-Tung University, Hsinchu, Taiwan, R.O.C., where she is currently working toward the Ph.D. degree.

Her research interests include the study of process techniques of VVCSELs.

**Jung-Tang Chu** was born in Taiwan, on July 12, 1978. He received the B.S. degree in physics from National Chung-Hsing University, Taichung, Taiwan, R.O.C., and the M.S. degree from the Institute of Electro-Optical Engineering, National Chiao-Tung University, Hsinchu, Taiwan, R.O.C., where he is currently working toward the Ph.D. degree at the Semiconductor Laser Technology Laboratory.

His research is focused on fabrication of III-V semiconductor light emitting devices.

**Min-Ying Tsai** received the B.S. degree in physics from Cheng Kung University, Tainan, Taiwan, R.O.C. She is currently working toward the M.S. degree at the Semiconductor Laser Technology Laboratory, Institute of Electro-Optical Engineering, National Chiao Tung University, Hsinchu, Taiwan.

Her research is focused on characterizing III-nitride and InGaAsN materials.

**Shing-Chung Wang** (M'79) received the B.S. degree from National Taiwan University, Taipei, Taiwan, R.O.C., in 1957, the M.S. degree from National Tohoku University, Sendai, Japan, in 1965, and the Ph.D. from Stanford University, Stanford, CA, in 1971, all in electrical engineering.

He has an extensive professional career both in academic and industrial research institutions. He has been a Faculty Member with National Chiao Tung University, Hsinchu, Taiwan, R.O.C. (1965–67); a Research Associate at Stanford University (1971–74); a Senior Research Scientist at Xerox Corporation, Palo Alto, CA, (1974–85); and a Consulting Scientist at Lockheed-Martin Palo Alto Research Laboratories (1985–95), Palo Alto, CA. In 1995, he rejoined National Chiao Tung University as a Faculty Member of the Institute of Electro-Optical Engineering. He has authored or co-authored over 160 publications. His current research interests include semiconductor lasers, vertical cavity surface emitting lasers, blue and UV lasers, quantum confined optoelectronic structures, optoelectronic materials, diode-pumped lasers, and semiconductor laser applications.